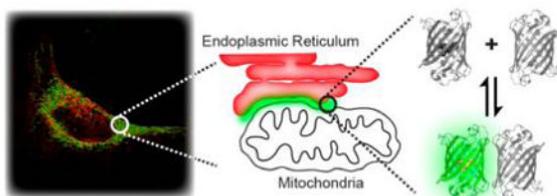# Dimerization-Dependent Green and Yellow Fluorescent Proteins

Spencer C. Alford[†,§], **Yidan Ding**[†,§], **Thomas Simmen**[‡], and **Robert E. Campbell**[†,*]

[†]Department of Chemistry, University of Alberta, Edmonton, Alberta T6G 2G2, Canada

[‡]Department of Cell Biology, Faculty of Medicine and Dentistry, University of Alberta, Edmonton, Alberta T6G 2G2, Canada

Abstract

Dimerization-dependent fluorescent proteins (ddFP) are a recently introduced class of genetically encoded reporters that can be used for the detection of protein interactions in live cells. The progenitor of this class of tools was a red fluorescent ddFP (ddRFP) derived from a homodimeric variant of *Discosoma* red fluorescent protein. Here, we describe the engineering and application of an expanded palette of ddFPs, which includes green (ddGFP) and yellow (ddYFP) variants. These optimized variants offer several advantages relative to ddRFP including increased *in vitro* contrast and brightness for ddGFP and increased brightness and a lowered pK_a for ddYFP. We demonstrate that both variants are useful as biosensors for protease activity in live cells. Using the ddGFP tool, we generated a highly effective indicator of endomembrane proximity that can be used to image the mitochondria-associated membrane (MAM) interface of endoplasmic reticulum (ER) and mitochondria.

Keywords

dimerization-dependent fluorescent protein; protein engineering; directed evolution; biosensor; caspase-3; mitochondria-associated membrane

Fluorescent proteins (FPs) and FP-based biosensors are an important class of genetically encoded analytical tools for life science research. Since the first example of recombinant expression of an FP nearly two decades ago,[1] the range of applications for FPs has steadily grown; FPs are now used in a wide variety of live cell molecular imaging applications[2]

including the determination of fusion protein localization, reporting of transcriptional activation, imaging of dynamic changes in small molecule concentrations, the visualization of enzymatic activities, and as a readout for synthetic gene regulatory networks.[3] Many of these applications are only made possible by the availability of FPs or FP-based tools engineered using a relatively small collection of well-established strategies.

In an effort to expand the range of FP-based tools, we recently developed a dimerization-dependent fluorescent protein (ddFP).[4] ddFP technology involves the reversible binding of two dark FP monomers to form a fluorescent heterodimeric complex (Scheme 1). The fluorogenic response associated with the FP–FP interaction is an indicator of an increase in the proximity or effective concentration of monomers. The initial example of a ddFP was a red fluorescent system (ddRFP) derived from dTomato.[5] The first generation construct, ddRFP-A_1B_1, is useful in a variety of applications, but it does suffer from limited brightness, limited contrast (~10-fold), and a limited color palette (only red).[4]

The goal of this work was to expand the color palette of ddFPs with variants exhibiting improved brightness and contrast relative to ddRFP-A_1B_1. Starting from the ddRFP template, we have used a process of directed evolution to create green (ddGFP) and yellow (ddYFP) analogues of ddRFP and explored their utility in live cell imaging applications. We found that while the low μM K_d of these ddFPs limits their utility in applications that involve free diffusion through the cytoplasm or within a single membrane, ddGFP is a useful reporter of endoplasmic reticulum (ER)-mitochondria contacts termed the mitochondria-associated membrane (MAM). Accordingly, we expect this expansion of the ddFP family of FPs to provide researchers with more color choices for development of fluorescent probes suitable for multiparameter imaging involving interactions between two biological membranes.

We have adopted the convention of designating the monomers of a ddFP as copy A (e.g., ddGFP-A) and copy B (e.g., ddGFP-B). The ddFP-A partner possesses the preformed, but quenched, chromophore, while the ddFP-B partner lacks a chromophore (Scheme 1).[4] We designate the noncovalent complex as AB (e.g., ddGFP-AB) and genetically fused tandem dimers with a "td" rather than the "dd" prefix (e.g., tdGFP-AB).

To generate new hues of ddFP, we chose to modify ddRFP[4] rather than repeat the directed evolution using a differently colored FP template. Our starting template for this effort was an unpublished ddRFP construct, ddRFP-$A_1B_{1.1}$ (Table S1, Supporting Information), that has a modest increase in contrast (~20-fold) and an increased affinity ($K_d \sim 1~\mu$M) relative to ddRFP-A_1B_1 (~10 fold contrast and $K_d \sim 30~\mu$M). Mutations K83R, K70M,[6,7] V105A, and V71M[8] have been previously reported to convert DsRed into a green FP. Various combinations of these mutations were introduced into the A copy of the tandem dimer version of ddRFP-$\mathbf{A_1B_{1.1}}$. The K83M and K70M mutations led to a complete loss of fluorescence, but dim green fluorescence was observed with the A71M (V71A arose during the evolution of dTomato from DsRed[5]) mutation independently or in conjunction with V105A (Figure S1, Supporting Information). The tdRFP-AB construct with mutations A71M or A71M/V105A in the A copy was used as the template for subsequent evolution.

Multiple rounds of library creation by error-prone mutagenesis followed by colony-based screening for high green fluorescence and diminished red fluorescence were undertaken.[9] In each round, the brightest variants were subjected to a secondary screen for contrast; the linker joining the two FPs in the tandem dimer was cleaved with trypsin, and the variants with the largest decrease in intensity due to dissociation were identified. Continued evolution with intermittent gene shuffling was continued until no further improvements were achieved during a round of exhaustive screening (Figure 1a). The brightest green fluorescent

variant (designated as tdGFP-AB) had 12 amino acid changes relative to ddRFP-A_1B_1 (Table S1, Supporting Information), with eight of these mutations in ddGFP-A and four in ddGFP-B.

The absorbance spectrum of purified tdGFP-AB is characterized by peaks centered at 380 and 493 nm (Figure 1b) and the absence of peaks in the red region (Figure S1, Supporting Information). Excitation at the 493 nm peak results in a green emission centered at 508 nm (Figure 1b). Excitation at the 380 nm peak results in weak (<0.1% relative to excitation of the 493 nm peak) emission peaks at 448 and 508 nm (Figure S1c, Supporting Information). The absorbance spectra of ddGFP-A and tdGFP-AB are pH dependent, with the 380 nm-absorbing species (acidic conditions) being converted to the 493 nm-absorbing species (basic conditions) with pK_a values of 9.4 and 7.8, respectively (Figure S2a–c, Supporting Information). Importantly, the brightness (Table S2, Supporting Information) and contrast of the green variant is improved relative to ddRFP-A_1B_1. Trypsinolysis of purified tdGFP-AB to disrupt the heterodimeric interaction (Figure 1c,d) produced a ~60-fold decrease in emission intensity (Figure 1d). This contrast is a marked improvement over ddRFP-A_1B_1, which exhibited a 10-fold increase in fluorescence upon heterodimerization.[4]

Given our success in evolving a green-hued ddFP, we next attempted to engineer a yellow-hued ddFP by introducing the mutation M66C, which leads to formation of a yellow fluorescent[10] three-ring chromophore.[11] Similar to the initial steps in ddGFP-AB engineering, installation of M66C into tdRFP-$A_1B_{1.1}$ decreased fluorescence intensity. Further molecular evolution ultimately produced an effective ddYFP-AB variant with 19 mutations relative to ddRFP-A_1B_1 (Table S1, Supporting Information) and good contrast in *E. coli* and *in vitro* (Figures 1e–h). TdYFP-AB exhibits absorbance and emission peaks centered at 520 and 546 nm, respectively (Figure 1f) and a 12-fold difference in emission intensity between the associated and unassociated states *in vitro* at pH 7.5 (Figure 1h). Although the brightness of this yellow variant is improved (Table S2, Supporting Information), its most promising feature is a reduced pK_a. At pH 7 ddYFP-A exhibits minimal absorbance at 516 nm (Figure S2d, Supporting Information), whereas tdYFP-AB absorbs near maximally and the protonated chromophore species is absent, consistent with the measured pK_a of 6.4 (Figure S2e, Supporting Information). Although this pK_a will render ddYFP-AB sensitive to pH fluctuations, it will retain ~75% of its maximum brightness at physiological pH (Figure S2f, Supporting Information). Conversely, the higher pK_a of ddGFP limits its brightness to ~25% of maximum at physiological pH (Figure S2c, Supporting Information).

In vitro saturation binding experiments revealed that ddGFP-AB has a K_d of 9 μM (Figure 2a) and ddYFP-AB has a K_d of 14.5 μM (Figure 2b), which both represent substantial decreases relative to the K_d of 33 μM for ddRFP-A_1B_1.[12] We speculated that the higher affinity could be attributed to the involvement of K153 in electrostatic interactions across the interface.[13] During the evolution of ddRFP-A_1B_1 we identified this residue as a modulator of heterodimer affinity.[4] Installation of the K153E mutation in ddGFP-B increased the K_d to 27 μM (Figure 2a) but reduced the brightness by ~30% and the contrast to ~37-fold (Table S2, Supporting Information).

We previously demonstrated that ddRFP-A_1B_1 is a suitable template for construction of genetically encoded biosensors for Ca^{2+} concentration and caspase-3 activation in live cells.[4] To assess whether ddGFP-AB and ddYFP-AB variants could also serve as templates for caspase-3 biosensors, we introduced a caspase-3 substrate sequence into the linker joining the heterodimer partners.[4] Expression of this construct in mammalian cells revealed that both tdGFP-AB and tdYFP-AB produce brighter fluorescence than tdRFP, though the brightest cells exhibited only small changes in intensity following caspase-mediated

cleavage (Figure S3a, Supporting Information). Presumably in these cells the concentration of tdGFP-AB is substantially greater than the ddGFP-AB K_d of 9 μM. In dim cells, which were presumably expressing lower levels of biosensor, we observed a 3.6 ± 1.0-fold ($N=$ 39) and 2.8 ± 0.6-fold ($N= 10$) decrease in fluorescence following caspase-mediated cleavage of tdGFP-AB and tdGFP-AB with K153E in the B-copy, respectively (Figure S3b, Supporting Information). The observed loss of fluorescence signal upon cleavage is reduced relative to the contrast observed *in vitro*. We speculate the concentration of monomers following cleavage is sufficient to cause noncovalent dimerization, and thus the observed contrast is decreased. Indeed, we find that coexpression of ddGFP-A and ddGFP-B in HeLa cells results in diffuse cytoplasmic fluorescence (Figure S4e, Supporting Information). For tdGFP-AB with K153E, the dimmer intrinsic brightness (Table S2, Supporting Information) requires us to image cells with a higher intracellular concentration, leading to increased dimerization and lowered contrast. For tdYFP-AB, caspase-3 activation traces were comparable in terms of kinetics and fold change to those obtained for tdGFP-AB-based biosensors (Figure S3c, Supporting Information).

On the basis of the results with the caspase-3 biosensors, it was apparent that the relatively high affinity of ddGFP-AB and ddYFP-AB would limit our ability to detect association or dissociation of proteins freely diffusing within the cytosol. We therefore explored the suitability of these tools for detection of protein proximity in cases where proteins are tethered to a membrane and thus not able to freely diffuse. We focused these efforts on ddGFP-AB because of its high contrast, and have not yet pursued the use of ddYFP-AB in similar applications. To determine if ddGFP-AB could be used to detect protein–protein proximity at the plasma membrane of mammalian cells, we fused ddGFP-A to a pleckstrin homology (PH) domain and installed a farnesylation substrate sequence on ddGFP-B.[14,15] We expected that the PH domain would recruit ddGFP-A to the membrane through association with inositol phospholipids[16] and farnesylated ddGFP-B would be tethered directly to the membrane (Figure S4a, Supporting Information). Indeed, prominent fluorescent labeling of the plasma membrane due to reconstitution of ddGFP-AB was observed only when both partners were targeted to the membrane (Figure S4b–d, Supporting Information), thus demonstrating the potential of our ddGFP heterodimers to detect protein proximity when anchored to a membrane.

We next tested the applicability of ddGFP-AB for labeling of the mitochondria–ER endomembrane contact sites called MAM.[17] Previous strategies to fluorescently image the MAM had used GFP-fusion proteins of MAM marker proteins, but these chimeras often did not fully reproduce targeting of the endogenous marker.[17] Our strategy was to coexpress ddGFP-A or -B chimeras in which each partner was fused to either the mitochondrial protein translocase of outer membrane-20 (Tom20) or the ER protein calnexin (Figure 3a). Tom20 is an outer membrane protein of the mitochondria that functions as a receptor during protein import,[18] and calnexin is a Ca^{2+} binding chaperone that is enriched on the MAM, where it regulates Ca^{2+} homeostasis.[19–21] We fused ddGFP-A to the C-terminus of calnexin and ddGFP-B to the C-terminus of Tom20 such that the ddGFP-AB partners are presented on the cytosolic face of the organelles (Figure 3a). When each gene fusion was expressed independently, no fluorescence labeling was detected above autofluorescence (Figure 3b,c). However, when both fusions were transfected, we observed prominent green fluorescence localized in the perinuclear region of cells (Figure 3d). The perinuclear localization was defined by discrete labeling at points of mitochondria–ER contact (Figure 3d) consistent with previous reports of MAM staining.[19,22] Parallel experiments were performed with two distinct ER targeting constructs that are not known to lead to MAM enrichment (residues 1–85 of *Rattus norvegicus* signal recognition particle receptor β (SRPβ)[23] and residues 1–218 of *Homo sapiens* B-cell lymphoma 2 (Bcl2) fused to cytochrome-b_5 (cb5) transmembrane domain[24,25]) and a mitochondria surface targeting domain (Bcl2 fused to the membrane

anchoring domain of actin assembly inducing protein (ActA)[24,25]). Expression of ddGFP-B fused to either the SRPβ or Bcl2/cb5 construct, together with ddGFP-A fused with Bcl2/ActA, gave no fluorescence signal above autofluorescence (data not shown).

To confirm that we were observing genuine MAM-mediated contact sites with the calnexin and Tom20 combination, we performed multiple control experiments. First, cotransfection with mCherry targeted to the mitochondria or ER demonstrated that the MAM-associated ddGFP-AB green fluorescence partially colocalized with both the mitochondria and the ER (Figure 4a,b; Figure S5a,b and S6a,b, Supporting Information). Second, to confirm that MAM labeling was dependent on the proximity of Tom20 and calnexin rather than the result of nonspecific ddGFP-AB aggregation, we utilized Tom20 mutants that have been reported to delocalize from the mitochondria.[26] Expression of these Tom20 mutants as mCherry fusions confirmed that these chimeras redistributed to the cytoplasm and Golgi (Figure S7a–i, Supporting Information). Fusion of these Tom20 mutants to ddGFP-B and coexpression with calnexin-ddGFP-A resulted in a loss of green fluorescent labeling of MAM interactions (Figure S8a,b, Supporting Information). As a final control, we cotransfected a knockout mouse embryonic fibroblast (MEF) cell line that is deficient for mitofusin-2, a protein that physically contributes to MAM contacts.[27] Transfected wild-type MEFs exhibited MAM labeling similar to that observed in HeLa cells (Figure 5a). In contrast, instances of MAM labeling were rarely observed in mitofusin-2 knockout MEFs (Figure 5b), and in those cases, the fluorescence intensity of the MAM label was diminished relative to WT MEFs. This result is consistent with impaired formation of ER-mitochondria membrane juxtaposition in MEFs lacking mitofusin-2.[27] Since MEFs are difficult to transfect,[28] we used flow cytometry to verify our observations made by epifluorescent microscopy (Figure S9, Supporting Information). Consistent with our imaging results, we observed an increase in the population of green fluorescent cells in wild-type MEFs relative to mitofusin-2 knockouts of 2.4 ± 0.8-fold ($N = 4$). Collectively, our results demonstrate that a ddFP approach using a MAM-enriched ER portion together with a mitochondrial portion provides an effective label of the MAM.

In conclusion, our work describes the engineering of new color variants of ddFPs, thus expanding the color palette of this FP class. We now have a series of ddFPs that possess a range of favorable features for live cell imaging: medium affinity and contrast (ddRFP), increased brightness and high *in vitro* contrast (ddGFP-AB), and increased brightness and reduced pK_a (ddYFP-AB). The availability of new color variants will better enable researchers to develop fluorescent probes tailored for specific imaging applications. However, the current ddFP series highlights both the potential and the challenges of using ddFPs as genetic parts for live cell biosensing. Specifically, each of the tools developed to date fall short of a being an ideal ddFP, which would be characterized by low affinity, low pK_a, high contrast, and high brightness. Further engineering efforts are likely to lead to ddFPs that are closer to ideal. Specifically, low affinity variants of the current ddFP family members will provide attractive alternatives to split-FP reporter strategies due to the reversibility of the intensiometric response. Our results with a MAM-specific ddGFP probe clearly show the potential of this new technology.

METHODS

Molecular Biology and Mutagenesis

All molecular biology reagents were purchased from Thermo Scientific/Fermentas. Error prone PCR was performed as described previously.[5] Gene shuffling mutagenesis was similarly conducted using template pools of either 5′ or 3′ genes of the tandem gene fusions and using short extension times (10 s) and increased cycle numbers.

Wavelength Selection and Library Screening with Tandem Heterodimers

Library screening was performed using our previously reported trypsinolysis assay.[4] Tandem heterodimers were initially constructed by a three-part ligation strategy that provided a chimera of the form A-linker-B in *XhoI/HindIII* sites of pBAD/His-B, where the linker was a 23-residue sequence that included a *KpnI* site. Bright colonies were picked and cultured in LB with ampicillin and L-arabinose (0.02%) overnight. Crude protein extracts were treated with trypsin at approximately 10 μg/mL for 30 min, and emission spectra were acquired using a 96-well microplate reader. Contrast ratios were calculated as the integrated emission peak area of the nontrypsinized extract divided by that of the trypsinized extract.

Hue-shifted emission wavelengths were selected using our custom-built colony imaging system; variants exhibiting favorable emission wavelength ratios (e.g., green-to-red) were confirmed by trypsinolysis assay and carried forward for further mutagenesis.

Protein Purification and Characterization

To produce recombinant proteins, the genes encoding tdGFP, ddGFP-A, and ddGFP-B were cloned into pBAD/His-B (Invitrogen). Expression plasmids were transformed in electrocompetent *E. coli* DH10B. Shaker cultures were induced at 0.02% L-arabinose and incubated a further 12–16 h. Soluble proteins were purified from cleared lysates by Nickel-NTA and buffer exchanged into 20 mM Tris-HCl, 100 mM NaCl and 0.5 mM EDTA, pH 7.5. pH sensitivity measurements were performed by incubating purified proteins in buffers of desired pH and acquiring emission spectra with a 96-well Safire2 microplate reader (Tecan). Spectra represented in this manuscript were recorded with a DU-800 UV–visible spectrophotometer (Beckman) or a QuantaMaster spectrofluorimeter (Photon Technology International, Inc.). The alkaline chromophore denaturation method was used to determine e values.[29] EGFP ($\Phi = 0.60$) or mCitrine ($\Phi = 0.76$) were used as the reference for quantum yield determination.

To determine the K_d of the purified recombinant ddGFP partners, an increasing amount of nonfluorescent ddGFP-B was mixed with a fixed amount of ddGFP-A to generate ddGFP-AB complexes in 20 mM Tris-HCl, 100 mM NaCl and 0.5 mM EDTA, pH 7.5. The integrated fluorescence emission peaks recorded as a function of ddGFP-B concentration were used to generate saturation binding curves. Experimental data was fit using a modified Langmuir isotherm to account for ligand depletion.

Live Cell Imaging

Caspase-3 biosensors were designed as described previously.[4] For membrane-targeting fusions the cDNA encoding the human Akt PH domain gene (residues 5–108) was fused at the N-terminus of ddGFP-A with an eight residue linker (GSSGTASS). The K-Ras farnesylation substrate sequence, SKDGKKKKKKSKTKCVIM, was installed at the C-terminus of ddGFP-B.[14] Each fusion was cloned into pcDNA3.1 (+) (Invitrogen) between *HindIII* and *XhoI* restriction sites.

Tom20 and ddGFP-B were fused with a short linker (GTASSEDNNMA) to render Tom20-ddGFP-B. Calnexin and ddGFP-A were fused together using the linker GGASGGSGSGPV to render calnexin-ddGFP-B. The following Tom20 mutants were generated: Tom20 (Δ25–51) as well as Tom20 (Δ34–51; K27S/R28S/R29S).[26] Each of these truncations was in turn fused to ddGFP-B. Localization markers were mCherry-mito-7 (mitochondria), mCherry-SiT-N-15 (Golgi), and ER (mCherry fused to calreticulin signal peptide and a KDEL retention sequence).

Cell Culture Experiments

HeLa cells, mouse embryonic fibroblasts (MEFs), and mitofusin-2 deficient MEFs were maintained in Dulbecco's Modified Eagle Medium (DMEM) supplemented with 10% fetal bovine serum and glutamax (Invitrogen) at 37 °C and 5% CO_2. Transient transfections of pcDNA3.1 (+) expression plasmids were performed using Turbofect (Thermoscientific/Fermentas). Twenty-four hours post-transfection, cells were imaged or analyzed by flow cytometry (BD Accuri C6 Flow Cytometer) in HEPES-buffered Hank's balanced salt solution.

Fluorescence Microscopy

Epifluorescent imaging data were collected using an inverted Nikon Eclipse Ti microscope equipped with a 150 W Lumen 200 metal halide lamp (Prior Scientific) and a 16-bit 512SC QuantEM CCD (Photometrics). Colocalization data was collected using a spinning-disk confocal Olympus IX-81 motorized microscope. Green and red excitations were conducted with 50mW 491 and 561 nm pumped diode lasers. LMM5 from Spectral Applied Research was used for laser merging. The two lasers were coupled to the spinning disk confocal head (CSU10; Yokogawa) mounted with a Sedat dichroic mirror (Semrock). The lasers were processed with appropriate filter sets (Semrock) to capture fluorescence images with an EMCCD (C9100–13, Hamamatsu), driven by Perkin-Elmer's Volocity software.

Supplementary Material

Refer to Web version on PubMed Central for supplementary material.

Acknowledgments

References

1. Chalfie M, Tu Y, Euskirchen G, Ward WW, Prasher DC. Green fluorescent protein as a marker for gene expression. Science. 1994; 263:802–805. [PubMed: 8303295]

2. Chudakov DM, Matz MV, Lukyanov S, Lukyanov KA. Fluorescent proteins and their applications in imaging living cells and tissues. Physiol Rev. 2010; 90:1103–1163. [PubMed: 20664080]

3. Purnick PE, Weiss R. The second wave of synthetic biology: from modules to systems. Nat Rev Mol Cell Biol. 2009; 10:410–422. [PubMed: 19461664]

4. Alford SC, Abdelfattah AS, Ding Y, Campbell RE. A fluorogenic red fluorescent protein heterodimer. Chem Biol. 2012; 19:353–360. [PubMed: 22444590]

5. Campbell RE, Tour O, Palmer AE, Steinbach PA, Baird GS, Zacharias DA, Tsien RY. A monomeric red fluorescent protein. Proc Natl Acad Sci U S A. 2002; 99:7877–7882. [PubMed: 12060735]

6. Baird GS, Zacharias DA, Tsien RY. Biochemistry, mutagenesis, and oligomerization of DsRed, a red fluorescent protein from coral. Proc Natl Acad Sci U S A. 2000; 97:11984–11989. [PubMed: 11050229]

7. Gross LA, Baird GS, Hoffman RC, Baldridge KK, Tsien RY. The structure of the chromophore within DsRed, a red fluorescent protein from coral. Proc Natl Acad Sci U S A. 2000; 97:11990–11995. [PubMed: 11050230]

8. Terskikh AV, Fradkov AF, Zaraisky AG, Kajava AV, Angres B. Analysis of DsRed Mutants. Space around the fluorophore accelerates fluorescence development. J Biol Chem. 2002; 277:7633–7636. [PubMed: 11773062]

9. Ai HW, Henderson JN, Remington SJ, Campbell RE. Directed evolution of a monomeric, bright and photostable version of Clavularia cyan fluorescent protein: structural characterization and applications in fluorescence imaging. Biochem J. 2006; 400:531–540. [PubMed: 16859491]

10. Shaner NC, Campbell RE, Steinbach PA, Giepmans BN, Palmer AE, Tsien RY. Improved monomeric red, orange and yellow fluorescent proteins derived from Discosoma sp. red fluorescent protein. Nat Biotechnol. 2004; 22:1567–1572. [PubMed: 15558047]

11. Kikuchi A, Fukumura E, Karasawa S, Mizuno H, Miyawaki A, Shiro Y. Structural characterization of a thiazoline-containing chromophore in an orange fluorescent protein, monomeric kusabira orange. Biochemistry. 2008; 47:11573–11580. [PubMed: 18844376]

12. Grefen C, Obrdlik P, Harter K. The determination of protein–protein interactions by the mating-based split-ubiquitin system (mbSUS). Methods Mol Biol. 2009; 479:217–233. [PubMed: 19083185]

13. Yarbrough D, Wachter RM, Kallio K, Matz MV, Remington SJ. Refined crystal structure of DsRed, a red fluorescent protein from coral, at 2.0-A resolution. Proc Natl Acad Sci U S A. 2001; 98:462–467. [PubMed: 11209050]

14. Cadwallader KA, Paterson H, Macdonald SG, Hancock JF. N-Terminally myristoylated Ras proteins require palmitoylation or a polybasic domain for plasma membrane localization. Mol Cell Biol. 1994; 14:4722–4730. [PubMed: 8007974]

15. Hancock JF, Cadwallader K, Paterson H, Marshall CJ. A CAAX or a CAAL motif and a second signal are sufficient for plasma membrane targeting of ras proteins. EMBO J. 1991; 10:4033–4039. [PubMed: 1756714]

16. Kavran JM, Klein DE, Lee A, Falasca M, Isakoff SJ, Skolnik EY, Lemmon MA. Specificity and promiscuity in phosphoinositide binding by pleckstrin homology domains. J Biol Chem. 1998; 273:30497–30508. [PubMed: 9804818]

17. Raturi A, Simmen T. Where the endoplasmic reticulum and the mitochondrion tie the knot: The mitochondria-associated membrane (MAM). Biochim Biophys Acta. 201210.1016/j.bbamcr. 2012.04.013

18. Baker MJ, Frazier AE, Gulbis JM, Ryan MT. Mitochondrial protein-import machinery: correlating structure with function. Trends Cell Biol. 2007; 17:456–464. [PubMed: 17825565]

19. Lynes EM, Bui M, Yap MC, Benson MD, Schneider B, Ellgaard L, Berthiaume LG, Simmen T. Palmitoylated TMX and calnexin target to the mitochondria-associated membrane. EMBO J. 2012; 31:457–470. [PubMed: 22045338]

20. Myhill N, Lynes EM, Nanji JA, Blagoveshchenskaya AD, Fei H, Carmine Simmen K, Cooper TJ, Thomas G, Simmen T. The subcellular distribution of calnexin is mediated by PACS-2. Mol Biol Cell. 2008; 19:2777–2788. [PubMed: 18417615]

21. Roderick HL, Lechleiter JD, Camacho P. Cytosolic phosphorylation of calnexin controls intracellular Ca(2+) oscillations via an interaction with SERCA2b. J Cell Biol. 2000; 149:1235–1248. [PubMed: 10851021]

22. De Vos KJ, Morotz GM, Stoica R, Tudor EL, Lau KF, Ackerley S, Warley A, Shaw CE, Miller CC. VAPB interacts with the mitochondrial protein PTPIP51 to regulate calcium homeostasis. Hum Mol Genet. 2012; 21:1299–1311. [PubMed: 22131369]

23. Ogg SC, Barz WP, Walter P. A functional GTPase domain, but not its transmembrane domain, is required for function of the SRP receptor beta-subunit. J Cell Biol. 1998; 142:341–354. [PubMed: 9679135]

24. Hwang YT, Pelitire SM, Henderson MP, Andrews DW, Dyer JM, Mullen RT. Novel targeting signals mediate the sorting of different isoforms of the tail-anchored membrane protein cytochrome b5 to either endoplasmic reticulum or mitochondria. Plant Cell. 2004; 16:3002–3019. [PubMed: 15486098]

25. Zhu W, Cowie A, Wasfy GW, Penn LZ, Leber B, Andrews DW. Bcl-2 mutants with restricted subcellular location reveal spatially distinct pathways for apoptosis in different cell types. EMBO J. 1996; 15:4130–4141. [PubMed: 8861942]

26. Kanaji S, Iwahashi J, Kida Y, Sakaguchi M, Mihara K. Characterization of the signal that directs Tom20 to the mitochondrial outer membrane. J Cell Biol. 2000; 151:277–288. [PubMed: 11038175]

27. de Brito OM, Scorrano L. Mitofusin 2 tethers endoplasmic reticulum to mitochondria. Nature. 2008; 456:605–610. [PubMed: 19052620]

28. Yamaguchi Y, Larkin D, Lara-Lemus R, Ramos-Castaneda J, Liu M, Arvan P. Endoplasmic reticulum (ER) chaperone regulation and survival of cells compensating for deficiency in the ER stress response kinase, PERK. J Biol Chem. 2008; 283:17020–17029. [PubMed: 18426796]

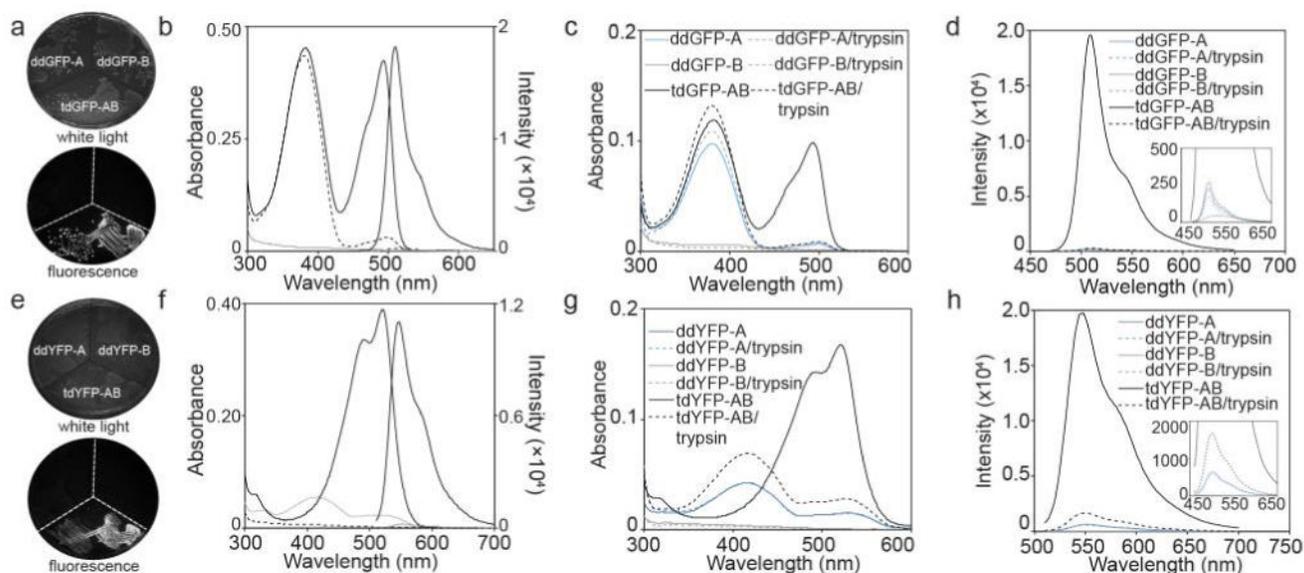29. Ward, WW. Properties of the Coelenterate Green-Fluorescent Proteins. Academic Press; New York: 1981.

Figure 1.
Spectral features and *in vitro* contrast of ddGFP and ddYFP. (a) *E. coli* expressing ddGFP-A, ddGFP-B, or tdGFP-AB. (b) Absorbance and emission of ddGFP-A (black dashed line), ddGFP-B (gray line), and tdGFP-AB (solid black line). (c) Absorbance and (d) emission profiles of tdGFP-AB and its monomers before and after trypsinolysis. Inset shows the low intensity fluorescence signal. (e) *E. coli* expressing ddYFP-A, ddYFP-B, or tdYFP-AB. (f) Absorbance and emission profiles of ddYFP-A (gray line), ddYFP-B (black dashed line), and tdYFP-AB (solid black line). (g) Absorbance and (h) emission profiles of tdYFP-AB and its monomers before and after trypsinolysis. Inset shows the low fluorescence intensity signal.
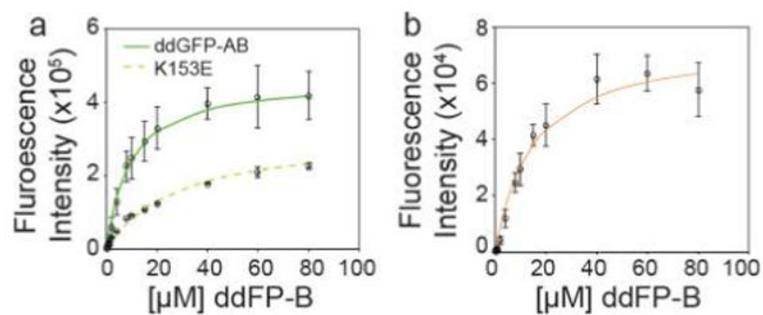
Figure 2.
Saturation binding curves for ddFP variants. (a) ddGFP-AB (solid green line) and ddGFP containing a K153E mutation in the ddGFP-B partner (dashed light green line). K_d values are 9 and 27 μM, respectively. (b) ddYFP-AB, K_d is 14.5 μM. Error bars are ± standard deviation for at least three independent experiments.
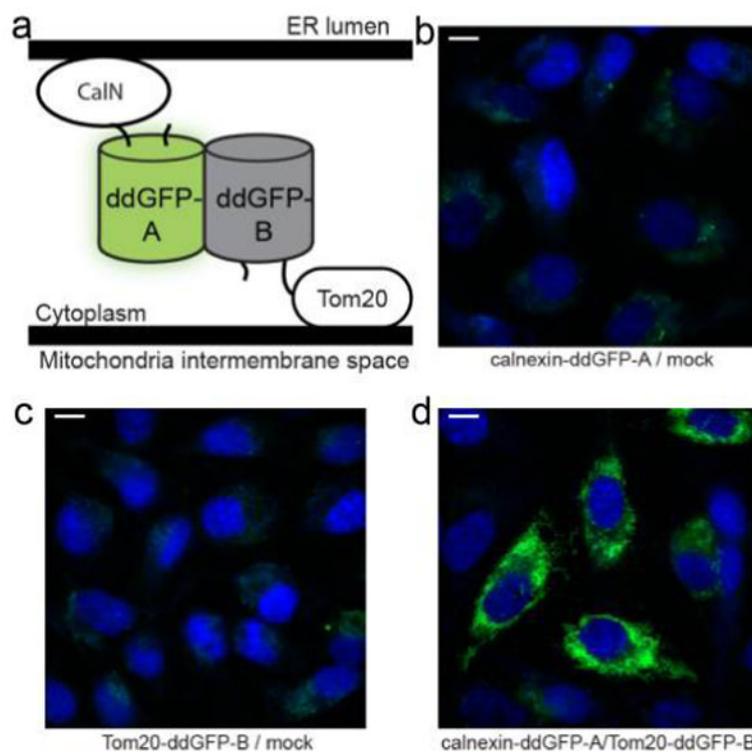
Figure 3.
ddGFP labeling of MAM in HeLa cells. (a) MAM labeling strategy. (b) Expression of calnexin-ddGFP-A or (c) Tom20-ddGFP-B alone. (d) Coexpression of calnexin-ddGFP-A and Tom20-ddGFP-B. Cell nuclei (blue) are stained with DAPI. Scale bars, 10 μm.
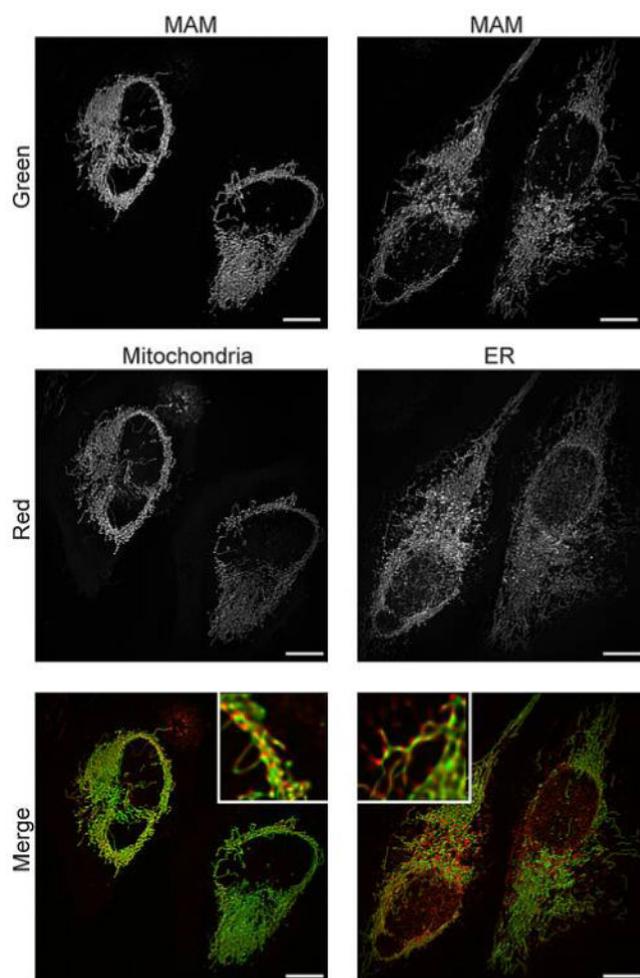
Figure 4.
ddGFP MAM label colocalizes with ER (right) and mitochondria (left). HeLa cells were transfected with three plasmids encoding calnexin-ddGFP-A, Tom20-ddGFP-B, and either a mCherry-ER or a mCherry-mitochondria marker. Top panel is ddGFP fluorescence, middle panel is red mCherry fluorescence, and bottom panel depicts merge. Images were acquired on an Olympus IX-81 motorized microscope spinning-disk confocal microscope. Scale bars, 10 μm.
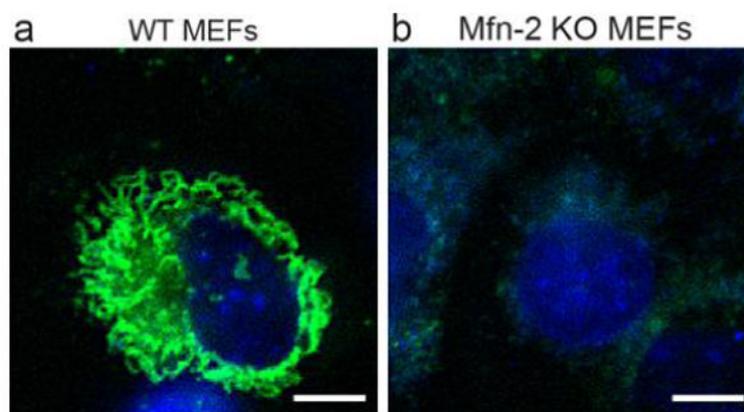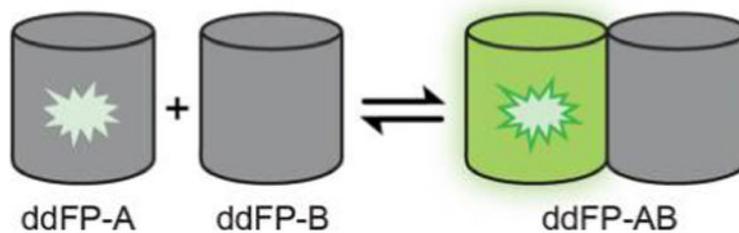
Figure 5.
The ddGFP probe is MAM-specific. (a) Wild-type (WT) or (b) mitofusin-2 knockout (Mfn-2 KO) MEFs cotransfected with calnexin-ddGFP-A and Tom20-ddGFP-B. Depicted are fluorescent images obtained for independent cotransfections. Cell nuclei (blue) are stained with DAPI. Scale bars, 10 μm.

Scheme 1. Conceptual Schematic of ddFP Technology[a]
[a]Weak or nonfluorescent protein monomers reversibly associate to form a fluorescent heterodimer. Chromophore indicated by starburst.